STEP

Subtitle

Student: **Marc Breiner Sørensen #201708238**
Supervisor: **Hans Kjeldsen**
Institut for Fysik og Astronomi, Aarhus Universitet

December 6, 2021

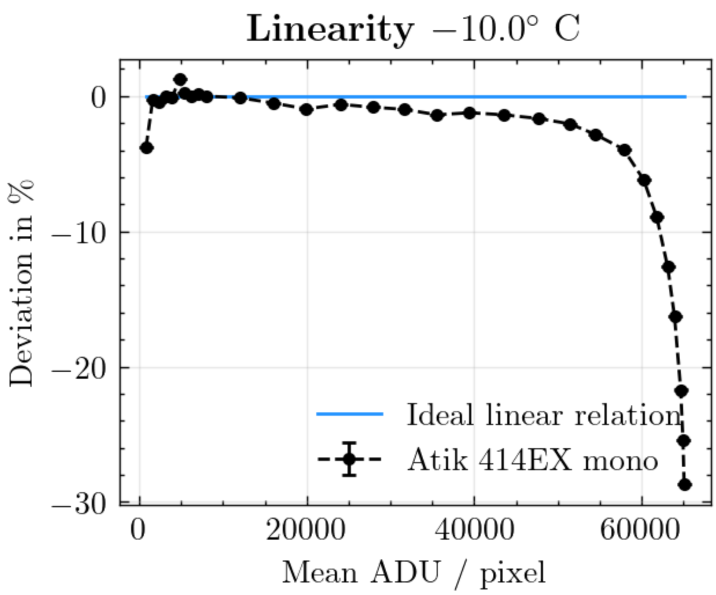

Contents

1

Abstract

2

Introduction

3

Detectors and their characterization

3.1 Charged-coupled devices (CCDs)

The detector that will be flown on the satellite is a light-sensitive detector, called a charged-coupled device (CCD). Such a detector is also referred to as a camera, and will in the present case be used to either do spectroscopy or image stars to look for exoplanets using the transit method. To formulate the scientific goals for the mission, and determine if we can fulfill them with a given camera, we must characterize the detector, and before we do that we should first understand how it works. This section will outline the basic physics of the CCD detector used in most digital cameras.

A CCD is a solid-state image sensor used to detect light. It is an integrated circuit that is essentially an array of metal-oxide-semiconductor (MOS) capacitors (MOSCAP) forming a photoactive region of silicon. Each of these MOSCAPs represents a pixel in the image. Understanding how the pixels work relies on a solid understanding of the semi-conductor which is described first. We may then describe the MOSCAP, which relies on the working principles of the pn-junction. To conclude, the readout of charge, which is what in the end will be interpreted as the image, is described.

3.1.1 Semiconductors

The photoactive region of the CCD, is an epitaxial[1] layer of silicon. Silicon is a semiconductor, which is a kind of solid-state material that has several useful properties when

[1] An epitaxial layer refers to a growth on top of a crystal or other material.

designing a detector. In order to understand the pixel of the CCD, we need to understand the interaction of light with the solid-state material.

A semiconductor is a type of solid-state material, which is neither a conductor nor an insulator. This distinction between insulators and conductors is defined from the difference in the density of states at the chemical potential at a temperature of $0K$[2]. For metals, we have a finite density of states. Otherwise, it is an insulator or a semiconductor. A semiconductor is a material for which the bandgap between the highest occupied states in the valence band, and the lowest unoccupied states in the conduction band, is sufficiently small, enabling thermal excitation of electrons across the gap. This gap is usually in the order of magnitude of a few electron volts.

A semiconductor is a solid, for which the chemical potential at absolute zero is placed at an energy level such that the density of states is zero. This is around the center of the bandgap. At finite temperature, some of the electrons from the valence band are thermally excited into the conduction band. This leaves behind so-called holes in the valence band. Holes are simply a convenient way to describe the absence of electrons, allowing us to treat them as positively charged quasiparticles. The movement of electrons through the valence band is permitted by the presence of holes, which in turn can be seen oppositely, as the movement of a hole in the opposite direction. Holes are hence charge carriers in the valence band allowing conduction. We call electrons and holes 'carriers', and the concentration of carriers are in part what determines the conduction properties of a material.

The concentration of carriers in an intrinsic semiconductor, that is pure, is too low to give an appreciable contribution to conduction properties. A way to circumvent this problem is by doping the semiconductor. This is a process in which we introduce impurities in the solid. These impurities, called dopants, can either function as donors, also called **n doping**, in which they can donate electrons to the solid, or as acceptors, also called **p doping**, in which they take electrons in turn producing a hole. N dopants are chosen such that, at not too high temperatures, the states lie just below the conduction band minimum (CBM), while the p dopant states are just above the valence band maximum (VBM). The physics of doped semiconductors is the basis of the **pn-junction** that makes up the MOSCAP.

3.1.2 The pn-junction

The MOSCAP is an example of a practical technological application of semiconductor physics based on the working principles of the pn-junction. It is sometimes also called a diode [2]. A description of this application allows us to understand how the interaction of light with the solid-state material, leads to charge generation in the pixel, which is ultimately read out and interpreted as contrast in an image.

The pn-junction is the boundary between regions of a p- and n-doped semiconductor. Such a region can be constructed by doping inhomogeneously. In the n-doped region, most donors are ionized, and the majority carriers are electrons, while in the p-doped region, acceptors are negatively charged, and the majority carriers are holes.

As the two regions are joined, electrons diffuse into the p-region and holes into the n-region leading to the recombination of electron-hole pairs as they meet. This gives rise to a region at the boundary, of immobile acceptors and donors, whose charge is not compensated by mobile charge carriers. We call this site the **depletion layer**. The thickness of this layer is around 0.1 to 1μm [2]. An electric field arises due to the presence of the immobile ionized donors and acceptors. The electric field points from the net-positively charged n-region into the negatively charged p-region, presenting an obstacle for holes to move from the p-region to the n-region. The depletion layer widens, and the field strength increases, until an equilibrium between the electromagnetic and diffusion forces is reached. There is hence a **diffusion current** across the region for those carriers with enough energy to overcome the opposing electric field, and a **drift current** due to the presence of the same field. The chemical potential in the p-doped region lies close to the VBM. In the n-doped region, it is close to the CBM [2] . However, if we apply a voltage across the depletion layer the equilibrium between these currents is broken such that a net current[2] is produced,

$$I = I_{\text{diffusion}} - I_{\text{drift}} = I_0 \left(e^{eV/k_B T} - 1 \right), \tag{1}$$

were V is the so-called **bias voltage**. This bias voltage is essentially what lets the diode function as a valve for the current, and in our case allows for the build up of charge in the pixel.

3.1.3 The MOS capacitor as the pixel

The MOSCAP is a part of the so-called MOSFET structure. A MOSFET is a type of transistor made from the principle of the pn-junction and is usually constructed from silicon. A MOSCAP is constructed by forming a layer of silicon dioxide on top of a p-doped semiconductor. On top of this, a metal or polycrystalline silicon is deposited, functioning as an electrode, also called the gate. This is the source of the bias voltage.

[2] A diode is a kind of electrical component that acts as a valve for the current in a circuit.

Silicon dioxide is a dielectric insulator, so this construction is akin to a planar capacitor. See figure 1.

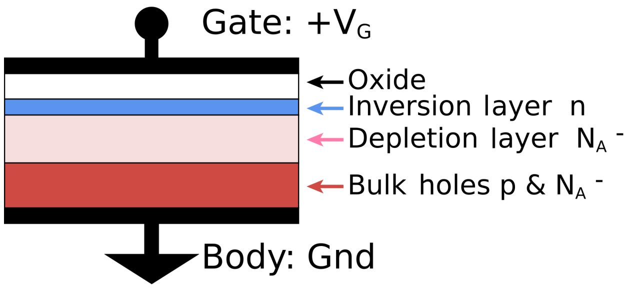

Figure 1: A MOS capacitor (MOSCAP). Image by Brews ohare Own work. Licensed under CC BY-SA 4.0, via Wikimedia Commons.

When a voltage is applied to the gate, holes in the body, the p-type substrate, will be repelled, and minority electrons will be attracted, generating a depletion layer underneath the oxide layer. If the voltage is great enough, enough electrons will be attracted, and electrons become the majority carriers, forming an n-type region. We call this layer an **inversion layer**. The threshold voltage at which this happens is an important parameter. It is defined as that voltage, at which the density of the electrons in the inversion layer is the same as that of the density of holes in the p-type substrate.

If in addition, two so-called **terminals** are included on either side of the body, consisting of n-doped regions (opposite type compared to the body type), the source, and the drain, we call the structure a **MOSFET**. In the case of a p-type (n-type) body, and two n-type (p-type) terminals, we denote it an nMOSFET (pMOSFET) or n-channel MOSFET. This makes up two pn-junctions. As voltage is applied to the gate and the inversion layer forms, a channel is formed that will allow current flow. The higher the voltage the greater the electron carrier density, and hence the greater the current flow between the two terminals. Transistors either amplify or switch electronic signals, and are essential building blocks in electronics.

3.1.4 CCD charge generation during exposure of the camera

We are now ready to describe charge generation in the CCD pixel. Before exposure of the CCD, the MOSCAPs in the array are biased into the depletion region, thus having not formed the inversion layer at this point. The gate is then biased positively (in n-channel MOSCAPS) above the threshold for inversion, creating an n-channel below the gate, just as in the MOSFET structure. Holes are pushed far into the body substrate, and no mobile electrons remain; the CCD is in a non-equilibrium state called **deep depletion**. Now the chip is ready to detect photons, and formally the exposure begins.

As photons strike the depletion region, an electron-hole pair is formed and separated by the electric field. Charge is hence accumulated at the surface. This charge generation process can occur until a new thermal equilibrium is reached, a state which we call **full well**. The full well is a saturation effect, after which electrons may spill into neighboring pixels. The latter effect is called bleeding. This does not necessarily coincide with digital saturation, at which conversion of the signal from a current to a digital signal, in the analogue-to-digital converter, saturates due to lack of available bits.

Electron-hole pairs may also be created by thermal excitations anywhere in the array, generating noise referred to as dark current. This effect is linear with time and follows a Poisson distribution since they are rarely occurring stochastic incidents. Dark may be corrected for and is a crucial part of the characterization procedure.

3.1.5 CCD charge transfer and image readout

After the phase of charge generation, usually called **exposure**, the accumulated charge must be read and interpreted as a digital signal in the computer. This digital signal should ultimately result in a value in each pixel. This is done by transferring the charge from the array, and sending the resulting electrical signal through an **analog-to-digital converter (ADC)** which will convert the analog signal of charges into a digitized signal that can be interpreted by a computer. This stage is called readout and happens on a line-by-line basis [3]. Rows are shifted down one at a time until they reach the **readout register** (the final row). Within each row, each pixel is read out sequentially.

Generally, during readout, the chip is exposed to light, and hence the shifting process should be very fast, to avoid smear in the image. This however poses another problem, as a faster readout process results in a higher noise level. This issue is solved in a **frame transfer CCD** by a shielded area of the chip, equal in size to the photosensitive area. The shielded area typically consists of a highly reflective material, such as aluminum. After exposure, the rows are rapidly shited into the shielded area, after which the necessary time to read out the measurements is available. In many cameras, this can also be achieved via a **mechanical shutter**. The camera used to develop the test procedure does not have a mechanical shutter, and we should hence characterize any potential time offset that may occur as a result of this.

Now that a full description of CCD physics, and how a photosensitive detector works, has been presented, the basis of the testing procedure will be presented in the next

[3] Here a line denotes a row in the CCD MOSCAP array

section.

3.2 Characterization of CCDs

In order to determine if a CCD can meet the specified scientific goals of a mission, it must first be characterized. A characterization procedure is to be developed, and the result of that procedure applied to a detector, is to be compared to the scientific goals. The central characterization metrics of a CCD detector will be outlined in the following section.

3.2.1 Gain

We shall begin by describing the most basic metric that related the digitized signal to the analog. The relationship between the number of electrons generated at the chip, and the actual pixel value in the image, is called **gain**[3]. This value is dependent on the software used to read out as well as the chip itself. As electrons are transferred out from the chip, they pass through an amplification stage, where a capacitor is charged. t'The voltage from this capacitor is passed through an **Analogue-to-digital converter (ADC)** which transforms the voltage signal into one that can be interpreted as a string of binary digits. This conversion is done by the software, and the resultant units are **Analogue-to-digital units (ADUs)**, which is ultimately the pixel value. At the ADC and software conversion levels we can scale the signal by an arbitrary factor, preserving the relative pixel values. This arbitrary scaling factor is exactly the gain. It can be expressed as

$$\text{gain} = \frac{\text{Number of electrons per pixel}}{\text{Number of counts per pixel}} \tag{2}$$

In each pixel bin on the chip, there is a maximum number of electrons that can be stored. This number is known as the **ful well capacity** of the chip. In addition, there is a maximum number that can be represented in the digitized signal, that depends on the number of available bits in the ADC. For a 16bit ADC, this number is $\text{ADU}_{\text{max, 16 bit}} = 2^{16} = 65563$. It is hence natural to choose the gain factor, such that the full well capacity, corresponds to the maximum digital value that we can store. This is not necessarily the case as doing so can be difficult, as it relies on knowing this parameter to sufficient precision.

3.2.2 Dark frames

An intermediate definition is needed before we move on to the effects that require us to study the inherent behavior of the chip when not exposed to light, such as noise. A dark frame is an image acquired while the chip is not exposed to incoming photons. Such a frame may be used to study dark current and readout noise effects in a CCD detector and is also used to construct the master bias frame discussed below.

3.2.3 Bias

Readout noise in the chip follows a gaussian distribution (see section 3.2.4.1) centered on zero. Hence there will be negative values in some of the pixels. To avoid negative counts in an image that consists entirely of noise, an offset voltage is applied to the CCD. This voltage offset level is called **bias**.

In general, bias is roughly constant across a chip, but it is common for the bias frame to show some level of structure in the chip. These structures can either be from the mechanical construction of the chip surface, from bad columns that may have a significantly higher offset than the rest of the chip, or resulting from the chip being made up of different sections that were constructed independently, and then later joined together.

Bad columns and sectors in the bias image are generally stable over a long time, and bias does not vary with time, and hence is independent of exposure time.

To study the bias level in the CCD, one may acquire an image with effectively zero exposure time[4]. In addition, this exposure should be a so-called **dark frame**. Such a frame is acquired in a dark setting such that no light reaches the chip during exposure or readout. Since the chip is initially discharged right before exposure, and then read out sequentially after the exposure has been completed, it is important to ensure that as few photons as possible reach the chip.

This bias voltage must be characterized by acquiring dark frames. Such a bias voltage should be subtracted from other images when analyzing data, since it is an effect that is artificially introduced.

3.2.4 Noise

For a CCD there are three main types of important noise that must be characterize. These are **Readout noise (RON)**, **Photonic noise** and thermal noise also called **dark current**. These three kinds of noise will be discussed in turn below.

[4] By effectively zero we mean, as short an exposure time, as is permitted by the camera at hand. Typically this value is in the range of about 0.001s, which is also the case for the camera used to develop the testing procedure.

3.2.4.1 Readout noise

Readout noise is the stochastic process associated with the amplification of the signal. It is introduced at the amplifier during the readout of the charge from the chip. It is usually quoted in terms of the number of an RMS number of electrons introduced per pixel upon readout [3]. Read noise cannot be eliminated, but it can be minimized.

There are two components to the phenomena. The first one is an introduction of uncertainty at the ADC level. The process of converting the analog signal to a digital one is not perfectly repeatable but is a distribution of possible answers centered on a mean value. The second component is extra electrons introduced by the electronics at work during readout. The width of the resultant additive distribution is interpreted as the readout noise, as a number of introduced electrons per pixel. The size and temperature of the amplifier contribute to this noise. Especially the temperature introduces as significant contribution due to thermal fluctuations.

Read-out noise follows a Gaussian distribution, and the width, that is the standard deviation of the distribution, is the read noise (in electrons) divided by the gain (in electrons per count). This can be seen by producing a histogram of the values in the master bias frame. It is seen that this distribution is gaussian with a mean value of the mean bias level offset, and a width corresponding to the readout noise. See figure 2.

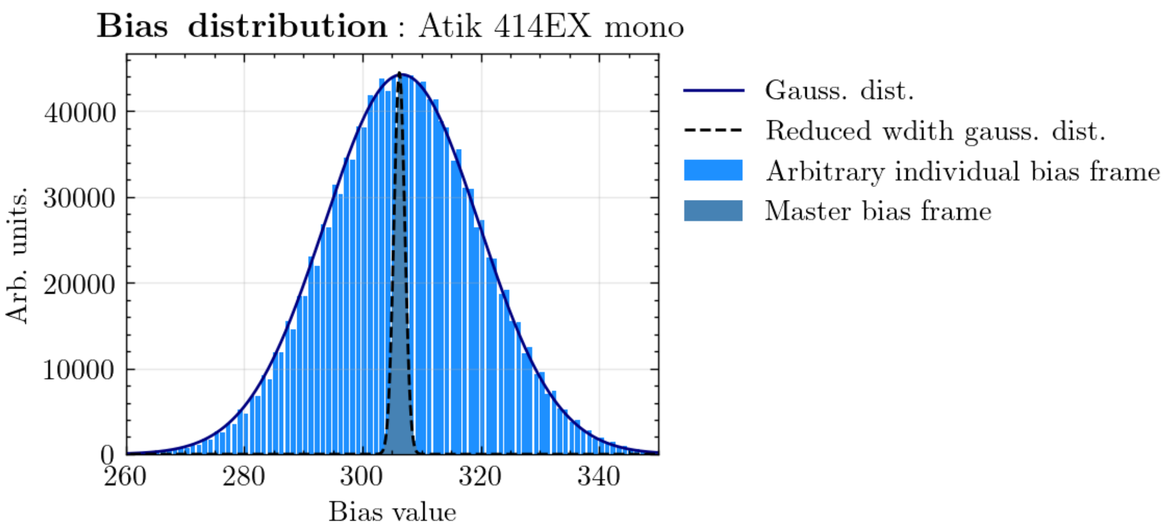

Figure 2:

Generally, a slower read-out speed will reduce the read-out noise [3]. This poses another complication, as a slower readout speed will introduce artifacts in the image, in the form of streaks, if the chip in question does not have a mechanical shutter.

3.2.4.2 Photonic noise

Photon noise is the natural variation, or in other words statistical fluctuation, of the photonic flux detected by the CCD. Photons detected follow a poisson distribution, since each photon is a discrete quanta, and the probability of the detection of the photon is independent of the other photons detected. A poisson distribution tends to that of normal distribution for large numbers, and hence the photon noise depends on the number of photons detected. We may hence reduce this photonic noise by observing bright objects that emit many photons, or by using longer exposure times.

3.2.4.3 Thermal noise and Dark current

Thermal noise, also called **dark current** is the resulting current in the chip, due to the thermal motion of the electrons in the solid-state material. This effect can be studied using the so-called **dark-frames** described above, in which the chip is not exposed to incoming photons, and hence no photo-electrons should be produced (in the ideal case of a perfectly dark room). The dark current depends linearly on time and is usually given as electrons per second. We thus obtain the following relation for the dark current in the chip

$$\text{dark current} = \frac{\text{ADU} \cdot \text{gain}}{\text{exposure time}}, \tag{3}$$

where the ADU value refers to the mean ADU / pixel in a dark frame. Gain is the detector gain described above. Thermal noise contaminates astronomical images making them hard to analyze and interpret scientifically, and should be eliminated. Fortunately, since dark current results from the thermal motion of electrons in the chip, it is strongly temperature-dependent and can be practically eliminated by cooling the chip. A well-designed testing procedure should characterize the dark current levels as a function of temperature. Readout noise levels are usually significantly greater than dark current levels, so dark frames must be taken at long exposure times, to yield an appreciably large dark current effect that can be practically isolated from that of the readout noise. This can also be achieved by averaging over a large number of dark frames, to average out readout noise. It should also be noted that a master bias frame should be subtracted from the dark fame to isolate dark current levels.

A master dark current frame can be constructed by averaging over many dark frames at a given exposure, subtracting the master bias frame, and then computing the dark current in each pixel according to equation 3. Such a frame can be seen in 3.

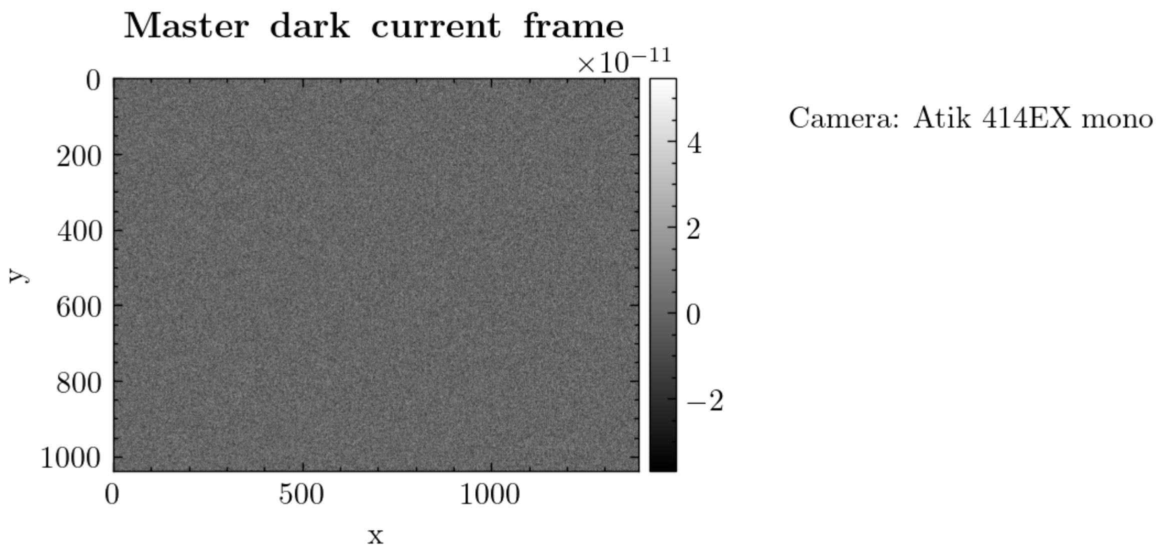

Figure 3: A master dark current frame constructed by averaging over many dark frames at a given exposure, subtracting the master bias frame, and then computing the dark current in each pixel according to equation 3.

3.2.5 Flat fielding

A CCD may not have a perfectly flat response to incoming light. By an ideal flat CCD detector, we mean a detector that uniformly detects photons with the same efficiency and sensitivity across the entire photo-active region of the chip. This ideal situation is seldom realized in practice due to faults in the chip or various manufacturing processes. Some CCDs may be constructed by joining several photo-sensitive pieces of silicon or may be constructed by grinding off layers of a block of silicon to achieve a thin detector. This grinding process may leave circular or straight lines through the chip that can be either more or less sensitive to light. There may also be specks of dust or fingerprints on the camera window causing blocking of light and diffraction patterns in the image.

In order to overcome this difficulty and to reconstruct the desired image from detector data in a non-flat CCD (which is usually the case at hand), we can utilize flat-field frames. Such frames are acquired by imaging a flat field, such as a white flat screen. Any non-uniformities in the resulting image, should, in the ideal experimental design, be due to the non-flatness of the chip, or obstructing objects on the camera window. This flat field frame then represents the relative light sensitivity between pixels in the chip. Construction of a master flat-field frame, by averaging over many such flat exposures, can then be used as a correction frame after normalizing it to unity. This is done by finding the greatest pixel ADU-value in the array and dividing the rest of the pixels in the frame by this value. This should be done after a hot pixel correction that will be described below. Now the master flat contains values in the interval (0, 1], the right end of the interval representing pixels that receive the most light. This frame can now be used for flat field corrections. This is done by dividing an image in question with the master flat on a pixel-by-pixel basis [5]. An example of such a master flat frame can be seen in figure 4.

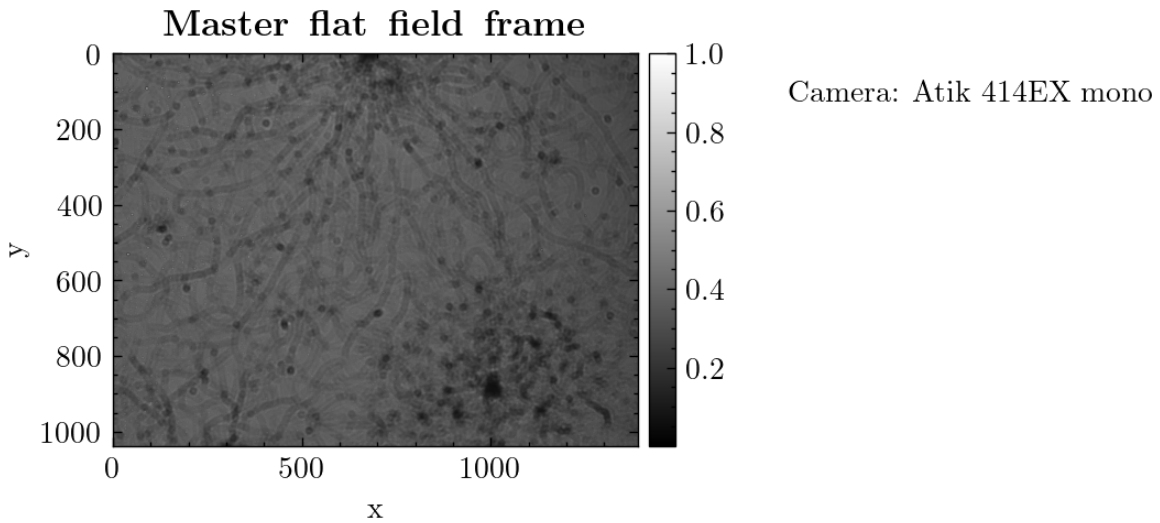

Figure 4: A master flat frame constructed by averaging over a given number of light exposures of a flat field, with 10s exposure times, subtrcting the bias and dark current master frames, and then normalizing to unity as described in section 3.2.5.

3.2.6 Hot pixels

A hot pixel is one which after an arbitrary exposure time, has an ADU value that is significantly greater than the mean value in the image. Such an effect can occur either because that pixel has a higher sensitivity to incoming photons due to the detector being struck by cosmic rays, or because the dark current in that pixel is higher and/or not proportional to time in a linear way. Dealing with cosmic rays is of particular importance for cameras in space since the rate of incidence is much higher than at the surface of the earth.

[5]Division by zero will not be a problem in practice, since generally there will always be a non-zero value in each pixel, for an arbitrary exposure time greater than bias, even after bias correction.

3.2.7 Linearity

Linearity is the response between measured ADUs and exposure time. In other words, if one doubles the exposure time, we expect to double the number of measured ADUs. We may study this effect by acquiring frames at different exposure times and comparing the mean ADU/pixel across exposure times. A detector is seldom perfectly linear, and the non-linearity must therefore be characterized. This is crucial for astronomical purposes since many observational metrics depend on the flux. In observing a star, using the passage method to detect exo-planets, the size of a planet can be estimated from the periodical dip in flux. If the detector, for a given exposure time (or equivalently ADU-range) is non-linear, the dip in flux will be affected, and the size of the planet may be larger or smaller.

The non-linearity of the detector may be defined as the deviation of a given measurement from the perfect linear behavior.

3.2.8 Charge diffusion and charge transfer efficiency

4

The test- and characterization procedure

4.1 Developing the characterization procedure

One goal of this work is to develop an experimental procedure, to characterize the camera that may be flown on the STEP mission. This characterization is crucial to test the validity of the scientific goals for the mission and should cover the metrics outlined in the preceding chapter. Such a procedure should be exactly reproducible, such that we can ensure its correctness. In this chapter, the initial considerations and the results from preliminary tests will be described. The conclusion that leads to the final measurement plan will then be presented.

4.1.1 The initial experimental setup for test plan development

The camera described in table 1 was used in the development of this testing and characterization procedure. The initial setup to carry out the testing and characterization procedure is seen in figure 5.

The setup consists of the camera resting on a stand, pointed into a white lacquered wooden screen. The camera is connected via USB2 to the lab computer and a power supply. Since the setup for dark frames requires a sufficiently dark room, an in-house darkroom is used. For all light exposures, the ambient room lighting was used, with the camera pointed into the screen. The ambient light is a double fluorescent bulb, and the light can be dimmed to roughly half of the flux by turning off half the bulbs. This is useful in order to control the length of exposure times during the acquisition of linearity data. To focus the light, and avoid rapid over-saturation, a pinhole was constructed from heavy

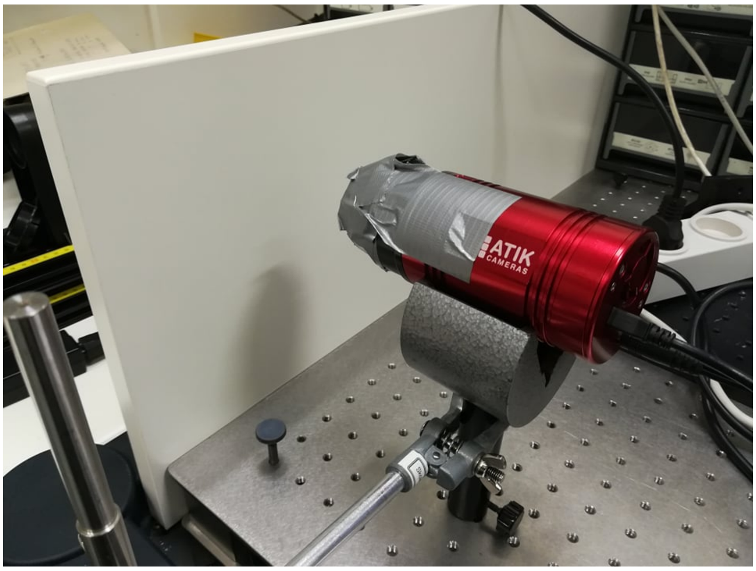

Figure 5: The initial experimental setup used both for the light and dark exposures. The setup consists of the test procedure camera resting on a stand. The camera is pointed into a white lacquered wooden screen, connected via USB2 to a lab computer, and a power supply. The setup is placed in a dark room to ensure we can acquire a proper dark frame.

Model name	Atik 414EX mono
Chip name	Sony ICX 825
Readout noise (typical)	$5e^-$
Gain factor	$0.28e^-/\text{ADU}$
Cooling ΔT	$-30°$
Dark current	$\sim 0.001e^-$ at $-10°$
ADC	16 bit
Pixel size	$6.45\mu m \times 6.45\mu m$
Shutter	No

Table 1: Relevant data specs for the **Atik 414EX mono** camera [1]

black cardboard and mounted with tape. For all dark frames, the same configuration was used, but with no ambient light, and computer screens turned off.

4.1.2 Preliminary thoughts and considerations

The starting point for the development of an experimental procedure will be outlined in this section. This is then tested experimentally, and from these results, the final procedure will be described.

4.1.2.1 Acquiring data and reducing noise

Characterization of a CCD chip involves acquiring images in a variety of ways to study several effects. Here, practical noise reduction steps that should be applied, will be described.

We acquire frames while varying a parameter like temperature (for thermal noise) or exposure time (for linearity). For each value of this varied parameter, say temperature for thermal noise (dark current), we wish to associate a functional value. In the case at hand, it is electrons per second. This is done by considering the frame taken at that value of the variable (temperature), and computing the mean value of the experimental metric (dark current, electrons per second) across all pixels in the image. For any measurement, we should take steps to reduce the noise in the image. Dark current can be reduced by cooling the chip before acquiring data frames. Readout noise is **gaussian** and the noise in the distribution is reduced by a factor of $1/\sqrt{N}$ for N measurements. Hence, for each datapoint, before computing the desired variable, like dark current for a specific temperature, we should, at that temperature, acquire N frames, and construct a mean image from these N frames. Typically N is chosen to be as large as is practically feasible. The value of the experimental metric is then computed from that average frame. Initially, $N = 100$ was chosen, but since, at ambient lighting levels used for the linearity measurements, longer exposure times make this impractical, $N = 10$ was chosen instead. The difference in the functional behavior of the curve, as a result of choosing a smaller value of N, was found to be of little importance. The temperature was chosen to be $T = -10^\circ$ C, due to reasons outlined in the next section.

4.1.2.2 Background noise and dark current

A good starting point for the development of the testing procedure originates from a preliminary investigation of the noise levels of the chip. This test was carried out at a desktop in an office, using a very primitive experimental setup. This preliminary test confirms that dark current is strongly dependent on temperature. See figure 6. Since the camera cooler can cool to a temperature gradient of $\Delta T = 30^\circ$C, the temperature $T = -10^\circ$ C was chosen. Since the cooling system works as a temperature gradient, it is

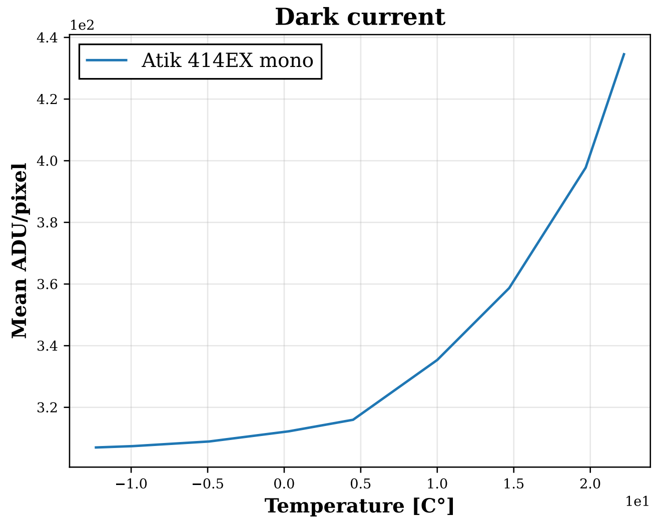

Figure 6: Preliminary dark current measurement, performed at the office in sub-optimal settings, to get a first glimpse of the behavior of this variable.

not feasible to go much lower. These steps ensure that we can minimize dark current and read-out noise.

4.1.2.3 Master bias and flat field frames

Bias images are frames with the smallest possible exposure time. This exposure time is $0.001s$ for the test procedure camera. Thus, for the construction of the master bias frame, we may choose N as large as$N = 300$. The bias frames are acquired in a dark setting with no light. This frame should be subtracted from all other data points. The same repeat number is chosen for the master flat-field frame, where the exposure time was chosen to be $10s$. The flat-field frames are acquired in a lit room setting.

For both the bias frames and the flat-field frames, we choose the $T = -10^\circ$ temperature setpoint chosen above, to reduce dark current.

4.1.2.4 Exposure times for linearity

The linearity measurement consists of acquiring exposures of the white screen, as a function of exposure time, in order to study the linearity of the response in measured photons by the detector. Hence we should first determine which exposure time interval to use. At first, a 100s exposure acquisition was carried out, in which considerable saturation was observed. From this, it was concluded that an exposure time of 100 seconds was a good datapoint to use for the last acquisition. This is true for the configuration in which all light bulbs were turned on in the room, representing the maximal flux achievable with this setup. The choice of exposure times generally relies on trial and error, to decide what range of exposure times we should use, at a given light source intensity. At first frames at exposures between $0.001s$ and $10s$ in $1s$, between $10s$ and 100s in $10s$ intervals, and $100s$ and $110s$ in $1s$ intervals was acquired. It was found that the light source stability varies slightly, resulting in greater uncertainty in short exposure measurements, and hence it was chosen to omit 0.001 seconds, and instead acquire frames in the interval $1s$ to $10s$ in 1-second intervals, in addition to the data sequence described just above. Due to the impracticality due to time constraints, of performing many measurements at long exposure times, it was instead chosen to acquire frames in the interval $10s$ to $110s$ in $5s$ intervals, which also samples the non-linearity curve better. Measurements with exposure times shorter than $10s$ are found to be more uncertain, see figure 7, likely due to a time offset resulting from the lack of shutter on the testing camera. The time calibration in question, which will be described below, poses difficulties. Hence it is recommended that a dimmer light source is used, and instead, frames are acquired at longer exposure times that pose lesser uncertainty in the measurements.

4.1.2.5 Noise as a function of temperature

Readout noise and dark current are expected to be temperature-dependent, and hence, in the entire cooling range of the camera, images of dark frames were acquired in order to study the behavior of these physical effects. Exposure times are chosen such that the minimal exposure time is chosen for the readout noise images since no photon should have been detected, and since the dark current is time-dependent, and hence should be negligible in this regime. For dark current frames, it is crucial to pick an exposure time such that the dark current contribution is greater (by a considerable amount, higher orders of magnitude) than the readout noise contribution. Dark current follows a **poissonian** distribution, and to recover this underlying distribution we should pick long exposure times. Since this requires **very** long times of exposure, it is more practical to pick an exposure time of $10s$, and then mean over $N = 100$ acquired images at this temperature, to reduce the noise contribution, since readout noise should be Gaussian with a zero-centered mean value.

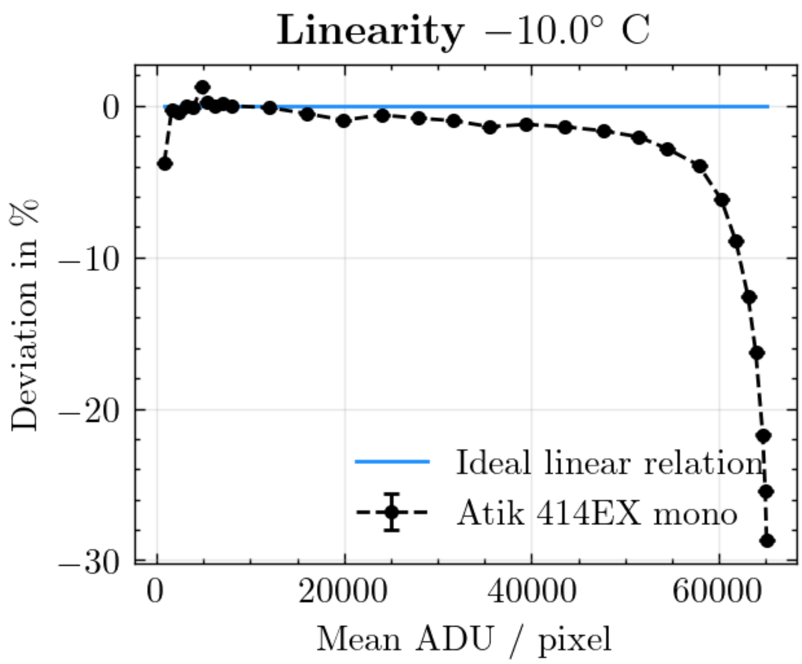

Figure 7: A plot of the percentage deviation from ideal linearity, computed according to equation 9 for each exposure time after meaning across N frames.

4.1.2.6 Hot pixel treatment

It is crucial to treat hot pixels. One way to do this is to realize that hot pixels are those pixels in which dark current does not show a linear temporal behavior. Acquiring a *very* long exposure, here chosen as a $1000s$ exposure, and a medium-long (considerably shorter than the former) exposure, here chosen to be a $90s$ exposure, we can study the dark current in each pixel, and determine if there is a linear relationship between the two frames.

Small values of the dark current are most accurately measured in the long exposure image, while the short exposure image will allow for the large dark current values to be accurately measured. We can not that for the test procedure camera, readout noise at $T = -10°$C, is around 3-4 electrons per image. Dividing that by the exposure time in the short exposure image, $90s$, corresponds to a dark current of about $0.33 - 0.44 e^-/\text{sec}$. It was noted that the dark current contribution should be significantly greater, for us to be able to see the Poissonian distribution of the thermal noise. Thus we may conclude that the smallest measurable dark current in that image will be around twice that [**?**]. We use this value as a filter, below which we do not include the pixel in the following treatment.

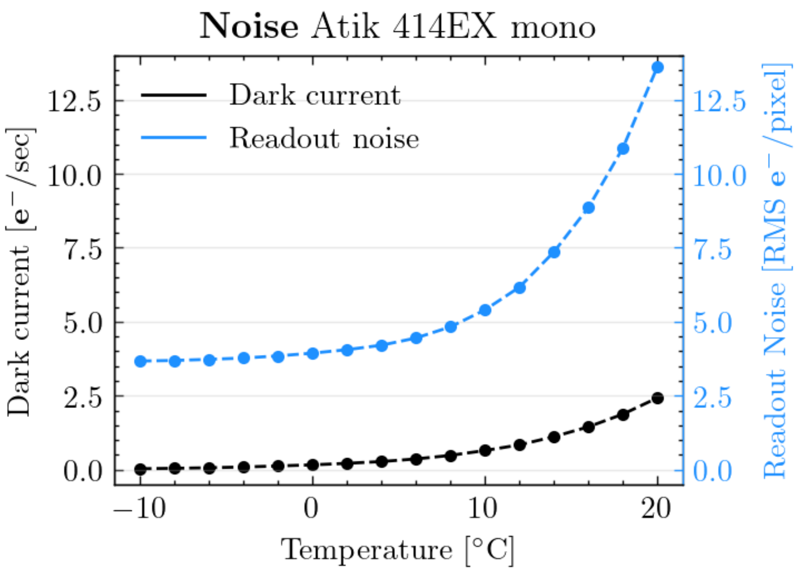

Figure 8: Dark current and readout noise as a function of temperature. The datapoints have been constructed by acquiring 100 dark frames at exposure times 0.001 s for readout noise, and 10s for dark current, at each temperature. Readout noise is computed according to section 4.2.3, and dark current according to equation 3.

By scatter plotting the pixels in the short exposure against the same pixels in the long exposure, and finding (qualitatively) the range within which the data points seem to follow a nice linear relationship. The remainder, that is those above a certain threshold beyond which they no longer appear to be linear, are considered hot in this sense, and from this information, a mask can be constructed. For the test procedure camera, this value is around a dark current of $7.5e^-/\text{sec}$. These pixels are then marked, and an image mask is formed. This mask marks which pixels to omit in the other analysis.

4.1.2.7 Testing of ground assumptions

In our experimental setup, assumptions have been made that need to be tested. The two most important ones, which enable the testing of linearity are that

- The camera has a well-calibrated zero-point temporally. That is to say that a 10-second exposure is physically the frame resulting from light being able to enter the chip for exactly 10 seconds. This is of particular importance since the camera used for the development of the testing procedure does not have a shutter.

- The ambient light source in the room is stable during exposure, so we can accurately compare ADU intensities between different frames. The ambient room light is used, which consists of double fluorescent light bulbs. We should as a null hypothesis expect to find fluctuations, and potentially even drifts in the light source over time.

The latter assumption can be tested by analyzing the many exposures taken during the first linearity sequence, by plotting the percentage deviation, from the mean ADU (mean across all $N = 100$ exposures at a given exposure time) as a function of exposure time. Both of these tests are outlined in the following two sections.

4.1.3 Stability of the lightsource

The experimental setup assumes the ideal case of a stable light source. This assumption should be tested, since we can generally not expect a fluorescent light bulb, connected to the main relay, to be stable to high precision. Preliminary investigations may utilize the wealth of data acquired during the linearity measurement sequence. At each exposure interval, $N = 100$ repeat frames were recorded. This enables us to plot the intensity as a function of time. From each repeat series, a mean image can be constructed. The mean ADU/pixel in this image is our reference value. The percentage deviation in the mean ADU/pixel, in each of the individual repeat frames, was then plotted as a function of time. This makes it possible to qualitatively judge the stability of the light source as a function of time. Such a plot can be seen in figure 9. Save for a few of the exposure times, the lighting is only stable to a few percentage points deviation. This yields a first estimate of the instability, indicating that we should correct this source of systematic error.

These deviations from perfect stability cannot be used as a correction, since this does not include the correlation of instability between exposure times. Instead, it is proposed that a reference exposure be utilized. Within a given repeat sequence, one may use a reference of $10s$ exposure by alternating between the chosen reference exposure, and the desired exposure time. Such an exposure series is akin to $[10s, 1s, 10s, 1s, 10s, \ldots 10s, 2s, 10s, 2s, \ldots]$ covering the entire range of exposure times. For each frame, we then have a 10-second exposure just before and right after. For the test procedure camera, the software designed for the camera only enables the user to set up a sequence of 10 data points to be acquired automatically but allows that sequence to be repeated. Hence it was most practical for the analysis to acquire data in the series $[10s, 1s, 10s, 2s, 10s, 3s, 10s, \ldots 10s, 9s, 10s]$, repeat that N times, and then repeat until the desired exposure time range has been covered. $N = 10$ was chosen due to time constraints. The two reference measurements to use in the correction of a given frame will then be the two taken at adjacent times.

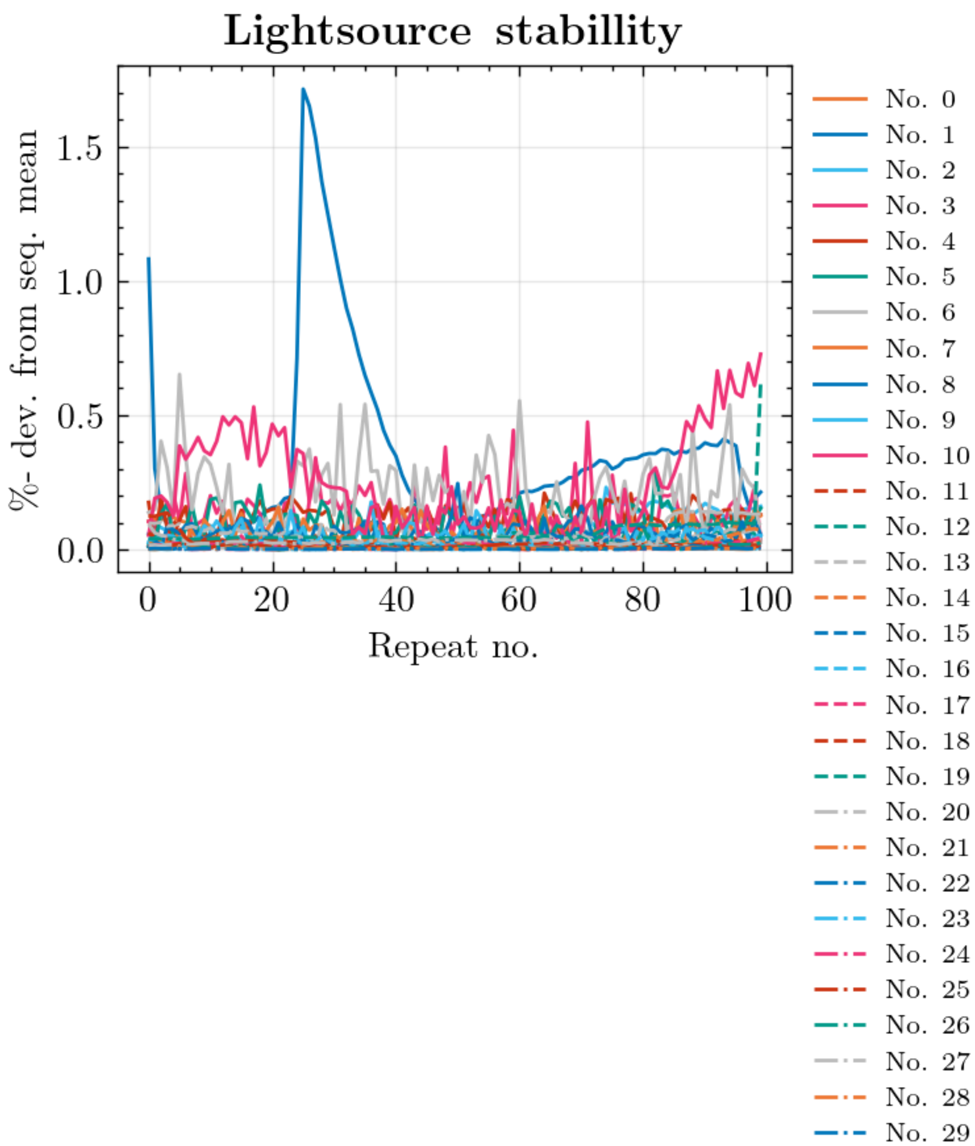

Figure 9: A plot of the temporal dependence in the lightsource intensity (flux) across each of the different exposure times. Numbering is ordered according to the preliminary series of exposure times as described in the text.

The flux of the light source at the time of our desired frame then lies somewhere in between, assuming no wild fluctuations or drifts, and a linear change in the time in between acquisition of the two reference frames. These assumptions of local monotonicity of the light source flux are justified by considering figure 9. In this way we are also able to correct for the potential long temporal drift of the intensity. Let $\boldsymbol{F}(x[s]) = \text{mean}\left(\text{Image}([s])\right)$ be interpreted as the mean flux in an image of exposure time s in seconds, that is, the mean ADU value of an arbitrary image of exposure time s. Hence we may correct for the instability, using a 10 second reference exposure, for a given frame via the computation

$$\boldsymbol{F}(x[s])_{\text{corrected}} = \frac{\boldsymbol{F}(x[s])}{\frac{1}{2}\left[\boldsymbol{F}(10s)_{\text{before}} + \boldsymbol{F}(10s)_{\text{after}}\right]} \cdot 10, \tag{4}$$

where the last factor of 10 is to account for the relation between the 10 seconds and 1 second exposure times, in the ideal case where there is no time offset.

4.1.4 Time calibration

Another assumption to be tested pertains to the camera itself: the time calibration of the measurements. A series of measurements were constructed to study if the zero-point was actually at $0s$ and to what precision. A preliminary estimate is gained by acquiring eight frames, noting that, under the assumption that our detector is linear, it should be true that for a given frame Image(Exposure time), we must expect for a perfect time calibration that

$$\frac{\text{Image}(21s) - \text{Image}(1s)}{\text{Image}(11s) - \text{Image}(1s)} = \frac{\text{Image}(10s) - \text{Bias}}{\text{Image}(20s) - \text{Bias}} \tag{5}$$

Or that

$$\frac{\textbf{mean}(\text{Image}(21s) - \text{Image}(1s))}{\textbf{mean}(\text{Image}(11s) - \text{Image}(1s))} - \frac{\textbf{mean}(\text{Image}(10s) - \text{Bias})}{\textbf{mean}(\text{Image}(20s) - \text{Bias})} = 0, \tag{6}$$

where **mean**() refers to the mean ADU/pixel within an image. The result of this, for the test procedure camera, being 0.0063 indicates a time offset which must be determined properly, and applied as a correction. The test procedure camera does not have a shutter, and the data sheet [1], specifies a $1/15s$ readout time. Hence an exposure time of $1s$ should correctly be interpreted as an exposure time of $1s + \Delta t$, where Δt should be deduced experimentally. Via a seperate linearity measurement series with greater precision (more datapoints) in the uncertain interval of $1s - 10s$, see figure 10 in which this readout

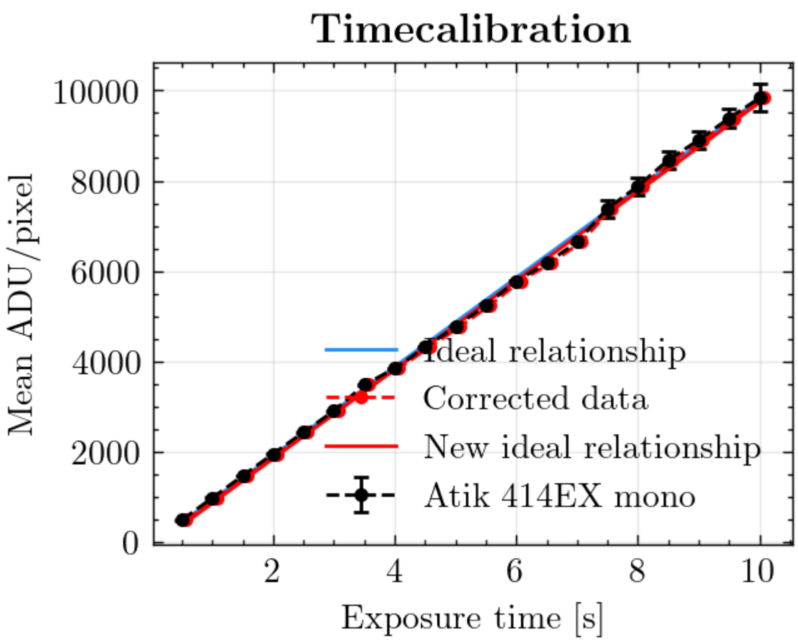

Figure 10:

time would actually be able to significantly impact exposure times, we can get a first estimate of Δt by fitting a linear function to the data points, and determining the roots of polynomium. If there is a time offset, the line will intersect the first axis at a point different from the origin. The intersection point on the first axis should be subtracted. For a negative value of the intersecting point on the first axis, a subtraction physically corresponds to a longer exposure time. In the same figure, the corrected data points are shown, along with the fit to the corrected data (in red). Deviations from the initial linear fit may be seen in figure 11, once again indicating that shorter exposure times are more uncertain.

Since we still observe fluctuations in the low exposure regime, we may try to circumvent the issue of fluctuations by using $1s$ exposure frames as a reference, by instead acquiring one $2s$ frame, "sandwiched" (in time) by two reference measurements of $1s$ exposure. Let us define $\boldsymbol{F}_A, \boldsymbol{F}_B$ to be the flux of the $1s$ reference frames that are taken respectively before and after the $2s$ frame, and correspondingly $\boldsymbol{F}_2$ the flux of the $2s$ frame. In that case the relation between the mean value of the flux before and after, to that of the flux of the $2s$ frame, which should be divided by 2 to correct for the double

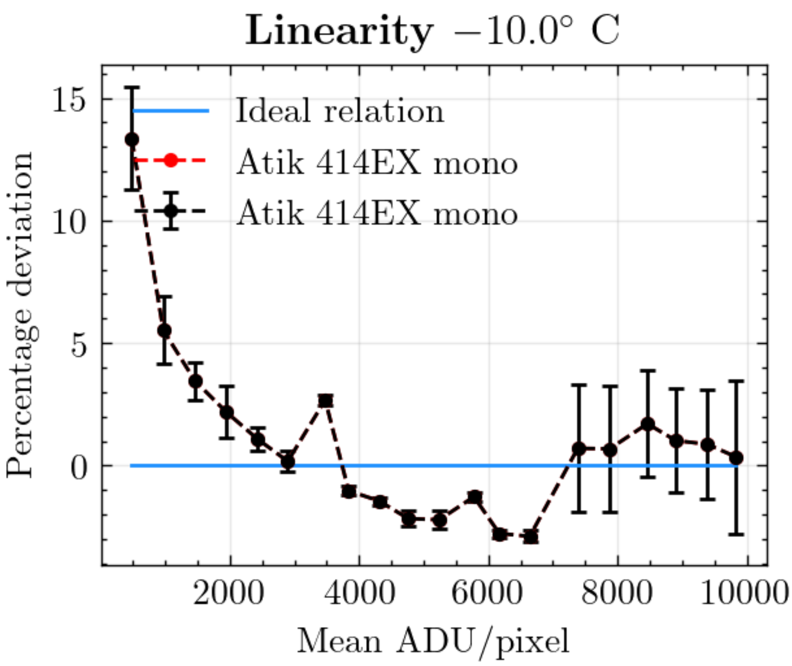

Figure 11:

exposure time, multiplied by the *true* exposure times, should be equal to unity

$$\frac{\frac{1}{2}(\boldsymbol{F}_A + \boldsymbol{F}_B)(1+\Delta t)}{\frac{1}{2}\boldsymbol{F}_2(2+\Delta t)} = 1 \tag{7}$$

Or, rearranging a bit, canceling the factors of $1/2$ and isolating for Δt yields

$$\Delta t = \frac{(\boldsymbol{F}_A + \boldsymbol{F}_B)/\boldsymbol{F}_2 - 2}{1 - (\boldsymbol{F}_A + \boldsymbol{F}_B)/\boldsymbol{F}_2} \tag{8}$$

We should then correct for this time offset by adjusting the equation 4, and achieving the same time the true measure of non-linearity, δ by subtracting 1 and converting to percentages as

$$\delta = \left(\frac{\boldsymbol{F}(x[s])}{\frac{1}{2}\left[\boldsymbol{F}(10s)_{\text{before}} + \boldsymbol{F}(10s)_{\text{after}}\right]} \frac{10s + \Delta t}{x[s] + \Delta t} - 1 \right) \cdot 100\%. \tag{9}$$

4.1.5 Linearity

The non-linearity, defined by equation 9, for data acquired in exposure times according to section 4.1.2.4, may be seen in figure 7. Consider the same figure, but zoomed in in

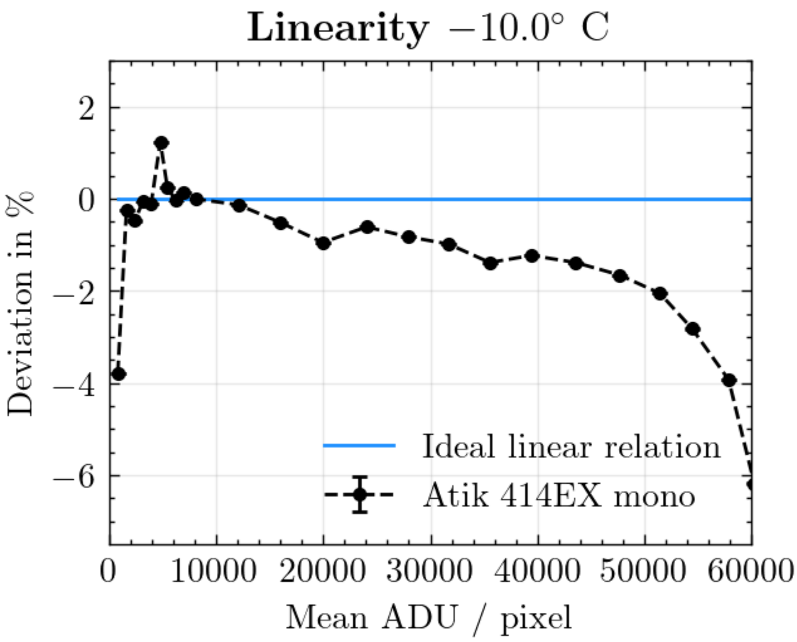

Figure 12: A plot of the percentage deviation from ideal linearity, computed from equation 9, but zoomed in.

figure 12. Perfect linear behavior is plotted as a blue line. Glancing at the graph we see there is an ADU interval, from around 0 to 45000 ADU, with the exception of a couple of datapoints, namely the first and the sixth. Whether the sixth datapoint is a statistical outlier, or a true peculiarity of the non-linearity curve, should be determined by a repeat of the experiment. Once again, fluctuations are observed in the low ADU regime, here corresponding to short exposure times in the interval between 1 seconds to 10 seconds. The latter is used as the reference exposure, which is why it correctly displays zero deviation. We may investigate if this is due to an incorrect estimate of the time offset, by varying it. In order to get a more precise estimate of the time offset from equation 8, we may, after correcting, interpret 9 as the true non-linearity, recognizing the low ADU datapoint deviations as imprecise. Fitting a linear curve to the data in figure 12, gives us a best estimate of the *true* linearity at the faulty points, which can be used to correct the fluxes in equation 8. This yields a new time offset, that may be reinserted in our analysis, and this process may be iterated until convergence.

In general it is recommended that the entire linearity curve is acquired at a dimmer light setting, such that the low-ADU regime does not correspond to short exposure times, and the time calibration is of lesser importance. Turning off 'half' of the flourescent light

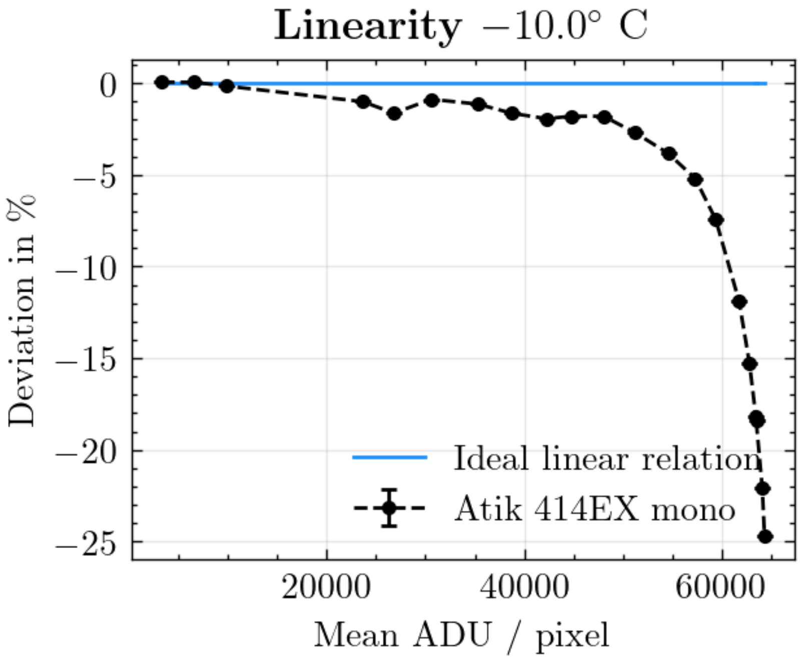

Figure 13: A plot of the percentage deviation from ideal linearity, computed from equation 9. Here the data is using a dimmer light source of roughly half the intensity, in order to decouple the low ADU regime from a low exposure time regime, such that the time offset becomes of lesser importance.

bulbs in the room, resulting in roughly half the intensity of light, cf. figure 13 and 14, confirms the suspection that fluctuations in the low ADU regime are due to the time offset. Now low ADUs correspond to longer exposure times, and the time offset is of lesser importance, since it corresponds to a much smaller fraction of the total exposure time. Our error is hence reduced significantly by choosing a dimmer light source. Qualitatively the non-linearity curve looks very similar, as it should, since in the ADU space we are independent of exposure times. For this data set the exposure times in exposure times $[10, 20, \ldots 230, 240]$, all in units of seconds, have been used. There were however faults in the series of $40s, 50s$ and $60s$, that have been omitted in the analysis. This was due to all of the lights having been turned on in the room by accident, during the acquisition of those datapoints.

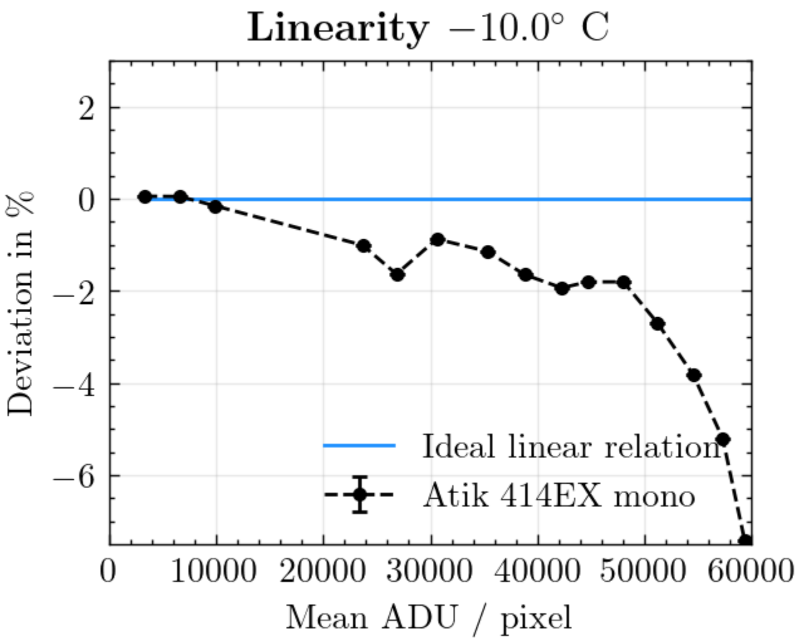

Figure 14: A plot of the percentage deviation from ideal linearity, computed from equation 9, with a dimmed lightsource of roughly half the intensity.

4.1.6 Shutter test

4.2 Measurement plan

This chapter will outline the test procedure measurement plan that results from the conclusions drawn in the preceding chapter. It will be presented as a step by step guide to obtaining the data.

4.2.1 Preparations and corrections

1. In a dark-room setting, acquire $N = 300$ repeats of $0.001s$ exposure images, mean over them to construct the master bias frame

2. In a lit-room setting acquire $N = 300$ $10s$ exposure images of the white screen, mean over them to construct the master flat field frame

3. In a lit room acquire frames at the exposure times $[0.5s, 1s, 1.5s, \ldots, 9s, 9.5s, 10s]$.

    - At each exposure time, acquire $N = 10$ repeats that will be meaned over.

- For each datapoint acquire a $10s$ reference measurement before and after, to correct for lightsource instability as according to the description outlined above
- For each exposure time construct a mean image from repeats
- For each of these mean images, one at every exposure time, and the reference measurements respectively before and after:
  - Subtract master bias frame from each of the three images.
  - Set hot pixels equal to mean value of the image, where hot pixels are omitted.
  - Compute the mean ADU/pixel in each image
  - Fit a linear relation to the data
  - Find the roots of the polynomium, which will be interpreted as the temporal offset due to the lack of a shutter

4.2.2 Linearity

1. Acquire frames at the exposure times $[10, 20, \dots 230, 240]$, all in units of seconds.
   - At each exposure time, acquire $N = 10$ repeats that will be meaned over.
   - For each datapoint acquire a $10s$ reference measurement before and after, to correct for lightsource instability as according to the description outlined above
2. For each exposure time construct a mean image from repeats
3. For each of these mean images, one at every exposure time, and the reference measurements respectively before and after:
   - Subtract master bias frame from each of the three images.
   - Set hot pixels equal to mean value of the image, where hot pixels are omitted.
   - Compute the mean ADU/pixel in each image
   - Compute the non-linearity according to equation 9

This produces a plot like figure 7

4.2.3 Temperature dependence of noise

For each temperature in the series $[-10, -8, -6, -4, -2, 0, 2, 4, 6, 8, 10, 12, 14, 16, 18, 20]$:

- 100 bias frames at 0.001s used to compute the readout noise as a function of temperature
  - At every temperature setpoint consider each repeat image in turn, compute the mean ADU/pixel and subtract it form every pixel in the image
  - The resultant image is a stochastic gaussian distribution with mean zero
  - Multiply every pixel with the camera gain, to convert to number of electrons.
  - Compute the standard deviation from the flattened array of pixels.
  - This yields 100 standard deviations, and from this a RMS value can be computed. These values can then be plotted as a function of temperature.
- 100 dark frames at 10.0s
  - For each temperature sequence, construct a mean image, in order to reduce the readout noise contamination in the image
  - Subtract the master bias frame.
  - Set hot pixels equal to mean value of the image, where hot pixels are omitted.
  - Multiply every pixel with the camera gain, to convert to number of electrons.
  - Divide every pixel with the exposure time
  - Compute mean ADU/pixel

The result of these two analysis may be seen plotted in figure 8

5

Results

6

Discussion

7

Conclusion

Bibliography

[1] Atik cameras spec sheets. `https://www.atik-cameras.com/specification-tables/`. Accessed: 8th October 2021.

[2] Philip Hoffmann. *Solid State Physics. An Introduction 2nd ed.* Wiley-VCH Berlin, 2015.

[3] S. Howell. *Handbook of CCD Astronomy*. Cambridge: Cambridge University Press, 2nd edition, 2006.